HUNTINGTON MEDICAL RESEARCH INSTITUTES
NEUROLOGICAL RESEARCH LABORATORY
734 Fairmount Avenue
Pasadena, California 91105

Contract No. NO1-NS-2333

QUARTERLY PROGRESS REPORT

April 1 - June 30, 1998

Report No. 11

"Microstimulation of the Lumbosacral Spinal Cord"

William F. Agnew, Ph.D.
Douglas B. McCreery, Ph.D.
Albert Lossinsky. Ph.D
Leo Bullara. B.A.

THIS QPR IS BEING SENT TO YOU BEFORE IT HAS BEEN REVIEWED BY THE STAFF OF THE NEURAL PROSTHESIS PROGRAM.

INTRODUCTION

We have been developing electrodes and protocols for safe, prolonged microstimulating in the mammalian central nervous system, using arrays of chronically-implanted microelectrodes. We have developed these methodologies to the point where microelectrodes can be implanted chronically into the feline cerebral cortex and into the cochlear nucleus of experimental animals with a minimum of tissue injury, and we have made considerable progress in the development of protocols for prolonged stimulation with arrays of closely-spaced microelectrodes. In the spinal cord, we have encountered some problems of electrode instability and tissue injury that appear to be related to the special environment of this site, and we have undertaken a series of studies to identify and remedy these problems.

One source of difficulty appears to be related to the rostral-caudal movement of the cord relative to the dura as the animal extends its hindlimbs or arches its back, and this may be linked to the manner in which the electrode cables are secured. The deformation of the tissue around the rigid microelectrode shafts during closure of the dura after electrode implantation may also contribute to the tissue injury. We have observed that the evoked responses recorded from the ventral roots and the elevations in bladder pressure induced by intraspinal microstimulation often change markedly after the dura is sutured over newly-implanted individual microelectrodes. This implies that the manipulation of the array during suturing of the dura may contribute to the displacement of the electrodes and hence to the tissue injury. However, the dura must be closed in some fashion to prevent leakage of CSF, and to keep the array from drifting up out of the cord. Also, the method of closure must not encourage the spinal roots or the subdural segment of the cable to become entrapped within connective tissue. Our 3-electrode arrays may be more stable during the suturing process than are the single microelectrodes that we have used previously, and we are investigating the merits of closing the dura with sutures after implantation of the electrode array and, alternatively, of patching the opening with a sheet of fascia.

In our first experience with chronic implantation of these 3-electrode arrays (QPR #10), the blunt-tipped electrodes remained in place, and induced minimal mechanical

injury to the parenchyma of the sacral spinal cord. However, the blunt electrode tips (radius of curvature of approximately 6 μm) did not easily penetrate through the tough pia near the dorsal root entry zone, and there was marked displacement and rotation of the cord as they were being inserted. This caused the electrode's trajectory to be considerably different from what was intended. There also were old glial scars adjacent to some of the microelectrode shafts, and this suggests that there was some slashing of the tissue during insertion of the electrodes, as would occur if the pia were to be displaced and distorted during electrode insertion. In two of the animals reported in this series (SP93 and SP94), the microelectrodes tips were somewhat sharper, fabricated with radii of curvature of 1.5 to 2 μm, in order to more easily penetrate the pia and thus produce less dimpling and rotation of the cord. We also report the findings from the final animal from the previous series (SP92), in which the electrode tips are very blunt (radius of curvature of ~ 12 μm). It is our experience that sharper microelectrodes with piercing tips tend to induce interstitial microhematomas in the cerebral cortex and in the cochlear nucleus and we are systematically examining this issue in the spinal cord.

METHODS

The arrays contain 3 activated iridium microelectrodes, staggered in length (1.2, 1.3 and 1.4 mm). The microelectrodes are 500 μm apart, and extend from an epoxy matrix 2 mm in length and approximately 0.75 mm in width. The microelectrodes themselves were 35 μm in diameter and were insulated with Epoxylite 6001 electrode varnish. In one cat (SP92), the tips were blunt (radius of curvature of 5 to 6 μm) in order to minimize injury to the microvasculature of the spinal cord. In two other cats (SP93 and SP94), the tips were sharper (radius of curvature of 1.5 to 2 μm), to reduce dimpling of the pia during insertion. These arrays did not have cables, since it is part of our strategy to examine the role of the cables in the displacement of the arrays. In the next (third) series of animals, the arrays will have cable, and we will examine two different means of stabilizing them, so that they do not dislodge the electrodes.

Three adult male cats (SP92, SP93 and SP94) were anesthetized with a mixture

of 50% nitrous oxide and 1.5-2.0% Halothane. The spinal cord was exposed from the L_6 to S_3 root level with a standard dorsal laminectomy. The dorsal spinal process anterior to the laminectomy was secured with a vertebral clamp. The S_2 level of the spinal cord is located by stimulating electrically the dermatome innervated by the S_2 root (the perigenital region) as a recording electrode was moved rostro-caudally over the dorsal surface of the cord. The position at which the maximum evoked response is recorded indicates the middle of the S_2 segment of the cord. A longitudinal incision was made through the dura at this level. The arachnoid was then dissected from the dorsal roots.

Two arrays of three iridium microelectrodes were implanted into each cat, using an axial introducer that was mounted to the frame securing the animal. The top of the array is held against the orifice of the introducer during insertion. The system is designed so that the electrodes can be inserted into the cord precisely on axis and thus minimize the chance of slashing the tissue. In cat SP92, the arrays of blunt-tipped microelectrodes were inserted into the dorsal columns at an angle of 26° from the vertical. In cats SP93 and SP94, the (somewhat sharper) electrodes were inserted vertically, through the dorsal root entry zone. In both cats, the target was the lateral cell column of the preganglionic, parasympathetic nucleus, which innervates the bladder detrusor muscle. In cat SP94, the system for localizing the S_2 segment did not function properly, and the electrodes were inserted slightly more rostrally, into the S_1 segment.

The spinal dura was not sutured closed after insertion of the arrays. A 8-0 monofilament suture was run between the left and right leaves of the dura, over the tops of the inserted array, and then tied loosely. This was done to hold the arrays in place, prior to their becoming encapsulated with connective tissue. Then, a patch of fascia was placed over the cord, prior to closing the musculature over the laminectomy. This healed quickly to the margins of the dura, and did not entrap the dorsal roots.

Thirty-five days after implantation of the arrays, the cats were sacrificed for histologic evaluation of the electrode sites. The animals were deeply anesthetized, then perfused through the aorta with saline followed by 1.5 liters of either ½ strength Karnovsky's fixative (SP93, SP94), or 4% formalin with 0.1% glutaraldehyde in 0.1 M

sodium phosphate buffer (SP92, for immunocytochemical studies). The sacral cord and spinal roots were dissected free, the connective tissue overlying the array matrices was shaved away, and the microelectrodes were removed from the cord. The surface of the arrays were exposed using either scalpel blades to trim away the surrounding tissues or, for cat SP92, a laser (YL5-1, Premier Laser Inc., Irvine, Ca.) was used to ablate the surrounding connective tissue. Due to technical difficulties, the lumbosacral spinal cord of cat SP94 was not properly perfused with the fixative. We decided to perform the autopsy immediately after perfusion. The entire spine was cut out using a Lipshaw Saw and immersion-fixed in ½ strength Karnovsky's Fixative. The fixative was placed into a 1L Erlenmeyer Flask with constant stirring for 48 hrs at 4° C.

The spinal cord was cut into segments, approximately 5 mm in length, and the tissue was embedded in paraffin, sectioned at 8 μm, and stained with hematoxylin and eosin. The primary goal of these studies is to assess the electrode's positional stability and the related tissue injury, and the thicker (8 μm) paraffin sections are more than adequate for this purpose. The use of paraffin embedding and the thicker sections considerably shorten the time required for histologic processing.

RESULTS

Gross Observations: In all three cats the three electrodes arrays were well positioned on the dorsal surface of the S_1 - S_3 region. The precise levels were determined by dissection of the spinal nerves.

Histologic Observations:

Histologic examination of the three animals enabled precise locations of the microelectrodes in animals SP92 and SP93. Because there were problems during perfusion of SP94, the spinal cord was not properly fixed. Consequently, due to *post mortem* hypoxic/ischemic effects, the structural integrity of the tissue was not optimum and the sites of the electrode tips in this animal were difficult to identify. We were, however, able to detect the depth to which all electrodes were implanted, with reasonable certainty. All electrodes in the three cats were observed within the medio-lateral gray matter. One electrode in cat SP94 left an "L"- shaped glial scar (Fig. 1). It

is possible that this electrode was mis-aligned prior to insertion, since the other two microelectrodes in the same array did not inflict scars.

A remarkable feature in all three animals was a meningeal inflammation (Fig. 2). The cells included mostly lymphocytes with a mixture of mononuclear cells, varying numbers of neutrophils and occasional multinucleated giant cells. In some cases, the meningitis appears to have spread down the capsule that encased the microelectrodes. In one animal (SP92) we noticed an organized, nodular-like lesion within the meninges. This nodule was composed of neutrophils, mononuclear cells and a few multinucleated giant cells, all of which were encased by lymphocytes (Fig. 3).

Inflammatory foci were seen within the parenchyma of the cord, and were primarily associated with the shafts of the microelectrodes, some distance from the tips (Fig. 4). It is not certain how this phenomenon is related to the meningeal inflammation described above. Some microelectrodes were unaffected and their histologic profile included the typical thin capsule ensheathing the shafts. The sheath is composed of fibrocytes, reactive glial cells with occasional multinucleated giant cells. Other major features observed in cats SP92 and SP93 included gliosis in the white matter associated with the inflammatory foci. There was vascular hyperplasia at all electrode tips, and there were few if any microhemorrhages. In animals SP92 and SP93, there were few if any neuronal changes (Fig 5). Because SP94 presented ischemic/hypoxic changes due to poor fixation, neurons exhibited a general darkening pattern with perineuronal halos and astrocytic edema, which masked any changes that might have been caused by the microelectrodes (Fig. 6).

DISCUSSION AND FUTURE PERSPECTIVES

These results indicate that discrete iridium microelectrodes with moderately blunt tips (with radii of curvature of 1.5 - 2 μm) can be inserted into the lumbosacral spinal cord with little trauma to the parenchyma of the cord. In particular, there is no evidence of an increased incidence of interstitial microhematomas, as we have observed in the cerebral cortex and in the cochlear nucleus when microelectrodes with very sharp tips

(radius of curvature of 0.5 μm) are implanted. Since the microelectrodes with radii of curvature of 1.5-2 μm are easier to insert through the dorsal root entry zone, we will use microelectodes with this tip diameter in the next series. The procedure of inserting the electrodes vertically while using the dorsal root entry zone as a surface landmark, in order to place the microelectrode tips into the lateral part of the intermediate horn, appears to work well.

One of the most interesting and disturbing histological finding in the three animals was the meningeal inflammation, and the sporadic presence of inflammatory foci along the shafts of the microelectrodes. Because not all of the electrodes were affected, the findings suggest a local stimulus. A large number of factors might be responsible for the inflammatory foci, but the most likely cause is a local irritant or toxin which is part of the composition of the electrode insulation. The matrices are composed of Masterbond epoxy, and the insulation around the iridium shafts is composed of Epoxylite 6001 varnish. Both are polymerized using baking schedules recommended by the manufacturers. However, the Epoxylite is cured using a schedule which, according to the data provided by the manufacturer, should be barely adequate to polymerize the material. This minimal schedule was chosen so as not to embrittle the insulation. If the epoxy monomers are not fully polymerized during the curing cycle, then monomers and oliogomers may leach from the insulation and cause a toxic irritation, which may stimulate local pro-inflammatory cytokine production, leading to leukocyte infiltrations. However, this does not account for the meningeal inflammation beneath the electrode matrices. It is also possible that contamination of the electrodes and/or their matrices by some bacterial or mycotic organism could also produce an inflammatory response, but this seems unlikely, since the electrodes are gas-sterilized prior to implantation.

We are aware that the inflammatory reactions are a potentially serious problem, particularly since it has been occurring more frequently during the past year, in the cerebral cortex, the cochlear nucleus, and now, in the spinal cord. We have modified the curing schedule for the Epoxylite varnish. The new schedule may cause the insulation to be somewhat more brittle, but should reduce the risk that the material is

incompletely cured. We have also modified the procedure for cleaning the complete arrays, prior to gas sterilization.

The observation of increased vascular hyperplasia near the electrode tips is also interesting. The hyperplasia occurs after implantation of most, if not all, microelectrodes into the brain, the cochlear nucleus, and the spinal cord, and resolves after 3-6 months. It is known that during angiogenesis, adhesion molecules up-regulate on their luminal surfaces. Adhesion molecules purportedly play a key role in facilitating leukocyte adhesion to endothelial cells. An increased density of adhesion molecules, therefore, may expedite the migration of blood-born leukocyte to specific blood vessels, prior to their emigration across the blood-spinal cord barrier. We are studying changes in the intercellular adhesion molecule adhesion molecule-1 (ICAM-1) during normal conditions and after electrical stimulation, in the brain and spinal cord of the cat.

In the next series, we will implant similar arrays with cable segments composed of pure platinum insulated with Teflon, to determine if the cables affect the arrays' mechanical stability. We will also continue immunocytochemical studies in an attempt to understand the nature of the inflammatory response that we have observed in recent animals.

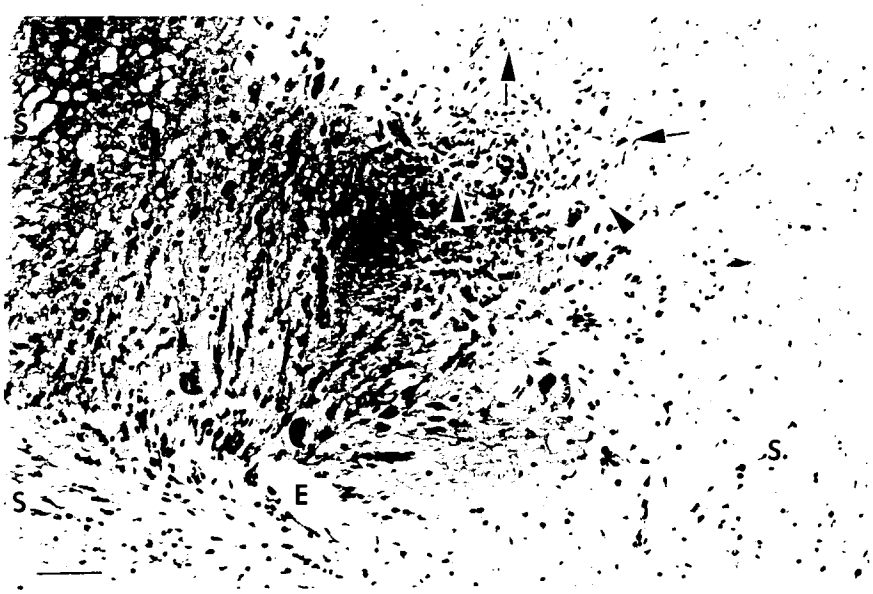

Fig. 1. SP94. The electrode track (E) is seen perpendicular to a sweeping scar in the center of the micrograph (*). The scar is composed of a mixture of lymphocytes (arrowheads) and reactive astrocytes (arrows). The spongy appearance of the white matter in the poorly perfused-fixed tissue in this animal is also shown (s). Bar = 100 μm.

Fig. 2. SP94. The meninges in the section of spinal cord demonstrates inflammatory foci surrounding several veins (*). Bar = 100 μm.

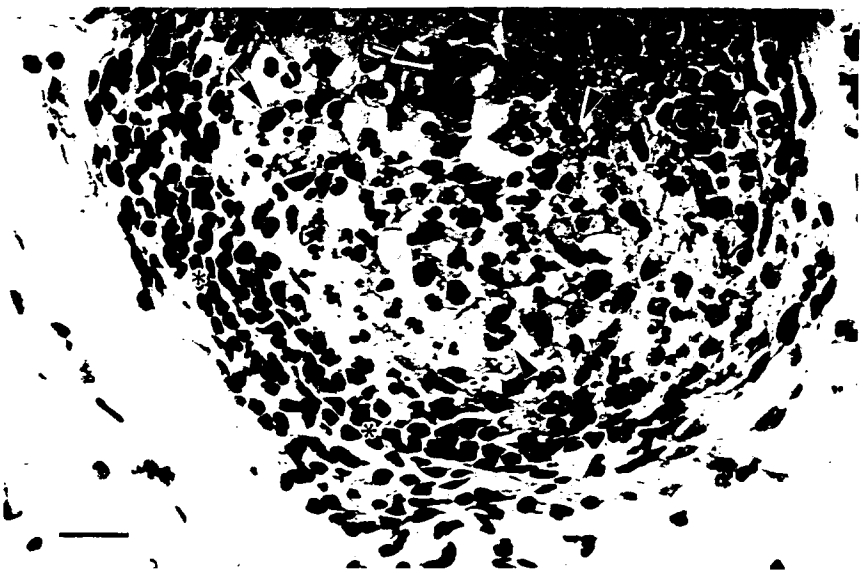

Fig. 3. SP92. The dorsal meninges contained a large, spherical area of inflammatory and connective tissue cells including neutrophils (arrowheads) and mononuclear cells (arrows) at the center, and a thick layer of lymphocytes at the periphery of this lesion (*). Bar = 50 μm.

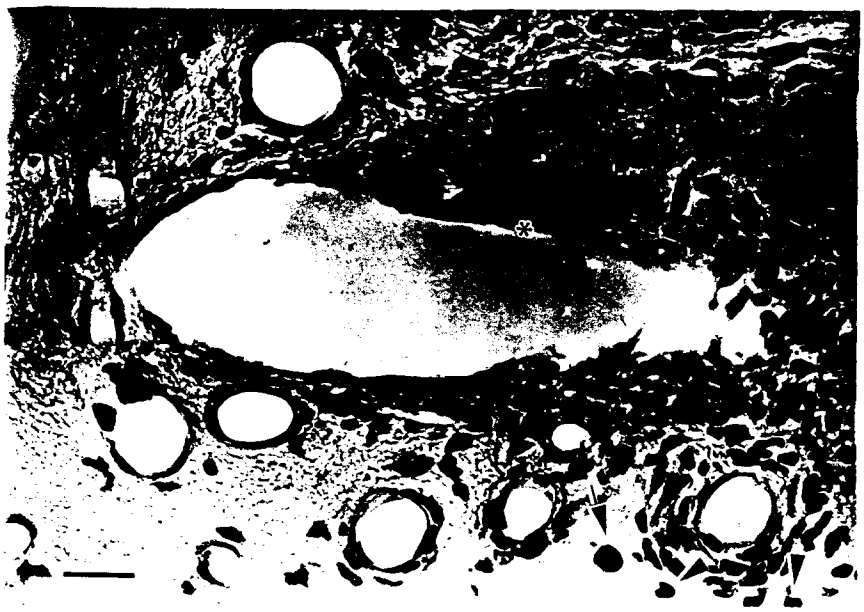

Fig 4. SP92. Some electrodes demonstrated a mild focus of mixed cells within or surrounding the electrode sheath that included multinucleated giant cell, granuloma-like structures (*), mononuclear cells (arrow) and few lymphocytes (arrowheads). Bar = 25 µm.

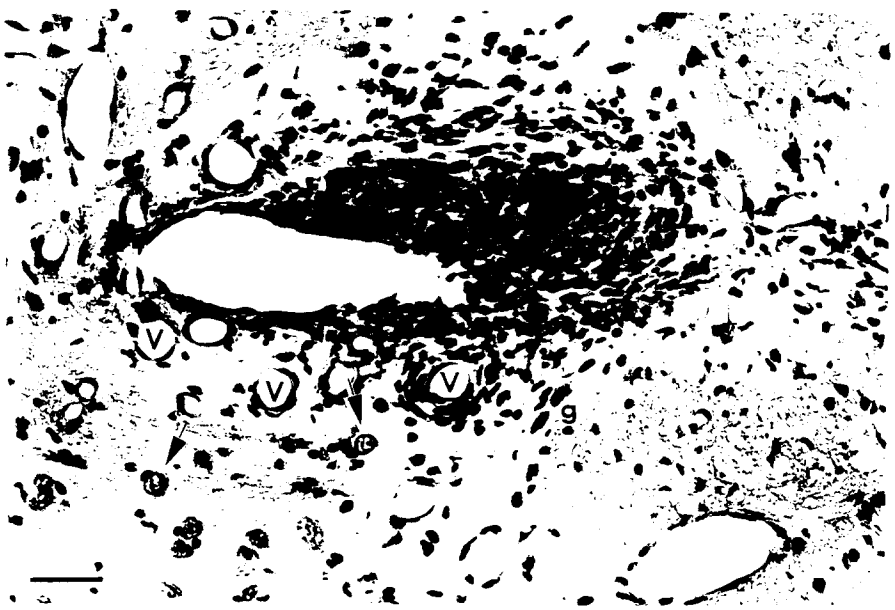

Fig. 5. SP93. Low magnification of Fig. 4. In most areas of the neuropil adjacent to the electrode sheaths, neurons appeared unaffected (arrows). Some gliosis (g) and vessel hyperplasia (v) is shown. Bar = 50 µm.

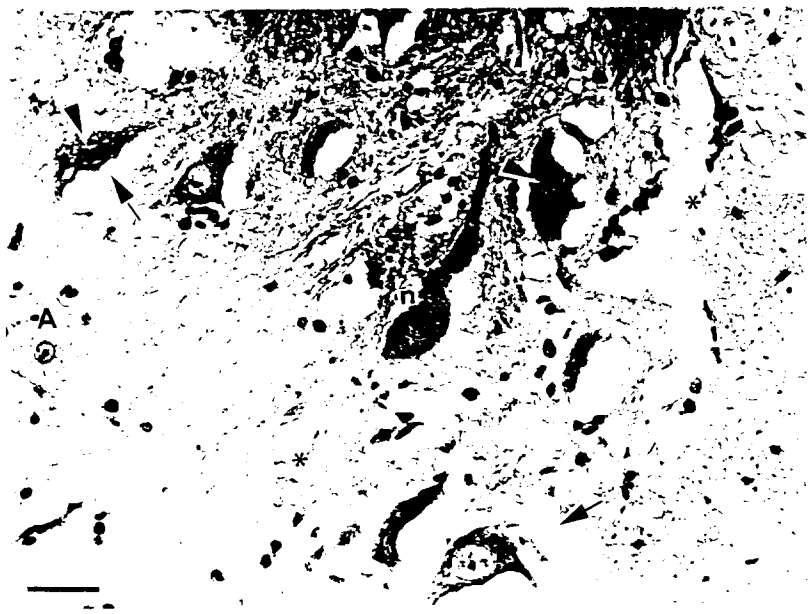

Fig. 6. SP94. Some of the hallmarks of hypoxic/ischemic injuries within the CNS include neuronal darkening and shrinkage (arrowheads), a watery appearance of the neuronal and other cell nuclei, perineuronal edema (arrows), astrocytic swelling (A), and increased spongy changes of the neuropil (*). Note the near normal appearance of one neuron (n). Bar = 50 μm.